

# A MODIFICATION OF THE PENROSE APERIODIC TILING

VIVIAN OLSIEWSKI HEALEY

## 1. INTRODUCTION

From black and white linoleum on the kitchen floor to magnificent Islamic mosaic to the intricate prints of M.C. Escher, tilings are an essential component of the decorative arts, and the complex mathematical structure behind them has intrigued scientists, mathematicians, and enthusiasts for centuries. Johannes Kepler, most famous for his laws of planetary motion, was known to have been interested in tilings, and his work was used centuries later when Roger Penrose extended one of his four hundred year old sets of tiles to form the famous Penrose tiles in 1976. Penrose's original aperiodic set contained six tiles, but his most well-known aperiodic set contains only two tiles.

The first known aperiodic set of tiles was discovered by Hao Wang. It contained more than 20,000 square tiles (now referred to as Wang tiles) with different edge colorings that were assembled without allowing rotations or reflections. However, the existence of sets of tiles that admit non-periodic tilings of the plane (tilings that possess no translational symmetry) was disputed until Robert Berger proved the undecidability of the domino problem (for Wang tiles) in 1966. The question of the domino problem was essentially whether there existed an algorithm to determine whether a set of tiles admitted a tiling of the plane. With the proposed algorithm, an aperiodic tiling would cause the algorithm to continue forever, so implicit in the problem was the question of whether aperiodic tilings of the plane existed. When Berger proved the undecidability of the domino problem, he proved the existence of aperiodic tilings.

These explorations were merely mathematical endeavors until 1984, when an experiment revealed a gaping hole in the classical theory of crystals. The result was a new theory of quasicrystals, which defined a class of crystalline solids that were capable of diffraction but did not possess translational symmetry. With the discovery of these structures, the mathematical study of aperiodic tilings became relevant to crystallography and physics.

In order to study these quasicrystals mathematically, they are modeled on tilings. From these tilings an "r-discrete" equivalence relation and the associated groupoid can be constructed. From here, the groupoid can further be given a (locally compact) topological structure, which in turn produces a groupoid  $C^*$ -algebra, in the sense described by J. Renault. Motivated by the "noncommutative geometry" program of A. Connes, J. Kellendonk later showed that when using the Penrose tilings to model quasicrystals, the elements of

---

<sup>1</sup>University of Notre Dame. E-mail: vhealey@nd.edu. Work produced with the guidance of Professor Terry Bisson and Professor B.J. Kahng under the NSF funding for the 2008 REU "Geometry and Physics on Graphs" at Canisius College.

this groupoid  $C^*$ -algebra may be regarded as physical observables of one or many-particle systems.

As one of the forms of the Penrose tiling has a three dimensional analogue that displays five-fold symmetry, the Penrose tiling is a widely used model of quasicrystals. For our purposes, we will consider a modification of the Penrose tiling discovered by Robert Ammann. This set of three prototiles admits only non-periodic tilings of the plane and does not require adjacency rules. No published work on the intricacies of this tiling could be found, and in what follows we explore the tiling, the construction of its appropriate r-discrete equivalence relation, and the associated r-discrete groupoid.

## 2. BACKGROUND

Here we explain the necessary mathematical concepts involving quasicrystals, groupoids, and tilings.

**2.1. Quasicrystals.** A crystal is a solid that is composed of identical units, which may be atoms, molecules, etc., in such a way that the units completely fill  $\mathbb{R}^3$ . Classically, a crystal is modeled by a lattice in  $\mathbb{R}^3$  by replacing each unit of the crystal by a point located at its center of mass. If any two points are equivalent under lattice-preserving translations, then the array is called a “point lattice” or “Bravais” lattice.

However, this theory of crystals is inadequate to describe the variety of crystal-like solids found in nature. Consider a classical Bravais lattice, and let the group of isometries that act on the lattice be called  $G_L$ . An element  $R \in G_L$  is restricted to have order 2,3,4, or 6 (Paterson, 163). Note that the order of the element refers to the number of copies of the element that must be composed to yield the identity element, or more simply, it is the number of times an isometry must act on the lattice to exactly return to the original configuration. (For a proof of the two dimensional case, see Patterson, 163.) One important shortcoming of this theory is that it excludes configurations with pentagonal or icosahedral symmetry. In 1984 it was discovered that the diffraction pattern of an alloy of aluminum and manganese displayed icosahedral symmetry (Paterson, 164). Crystal-like solids such as this one have come to be called “quasicrystals.” The symmetry of quasicrystals is best analyzed using groupoids, not groups, and instead of point lattices, quasicrystals are best modeled using “quasilattices” (infinite tilings of  $\mathbb{R}^2$  or  $\mathbb{R}^3$  formed from a finite number of distinct tiles).

(Paterson, 162-5)

**2.2. Groupoids and r-discrete Groupoids.** Roughly speaking, a groupoid as a generalization of a group with a partially defined multiplication. Below, we will briefly define the structure of a groupoid, but for further detail, we refer the reader to R. Brown’s text, *Topology and Groupoids* and A.L.T. Paterson’s text, *Groupoids, Inverse Semigroups, and their Operator Algebras*.

A groupoid  $G$  is defined over a set  $X$  and consists of objects that can be thought of as arrows from a source element in  $X$  to a target element in  $X$ . Let  $g \in G$  such that  $g$  has source  $y$  and target  $x$ . Then we define  $d(g) = y$ , and  $r(g) = x$ . We call  $d$  the source map and



FIGURE 1

$r$  the target map. Given two elements  $g, h \in G$ ,  $g$  and  $h$  are composable whenever the target of  $h$  equals the source of  $g$ . (An intuitive way to think about this is to consider connecting flights; a flight from New York to Washington can connect with a flight from Washington to Los Angeles but not with a flight from Boston to San Francisco.) That is, multiplication is only defined on the set of composable pairs:  $G^{(2)} = \{(g, h) \in G \times G \mid d(g) = r(h)\}$ . This multiplication is associative.

For the elements of  $X$  we have an embedding called the identity section which is a mapping  $\epsilon : X \rightarrow G$  such that  $\epsilon(r(g))g = g = g\epsilon(d(g))$ . Also, there is an inversion map  $\iota : G \rightarrow G$  such that  $\iota(g)g = \epsilon(d(g))$  and  $g\iota(g) = \epsilon(r(g))$ .

We note that a groupoid is essentially a category with inverses and also that a group is a groupoid where the set  $X$  contains only one element (multiplication is fully defined, since all pairs of elements are composable).

Often, a groupoid  $G$  can also be given a topology such that it is locally compact. Let  $G^{op}$  be the family of open Hausdorff subsets  $U$  of  $G$  such that  $r|_U$  and  $d|_U$  are homeomorphic onto open subsets of  $G$ . We say that  $G$  is  $r$ -discrete if  $G^{op}$  is a basis for the topology. Also, let an  $r$ -fiber of  $u$ , denoted  $G^u$  be the set  $\{u \in X \mid r(x) = u\}$ . If  $G$  is  $r$ -discrete, then it is known that its  $r$ -fibers are discrete. For more information on  $r$ -discrete groupoids, we refer the reader to Paterson's text.

**2.3. What Is a Tiling?** The following definitions have been adapted from *Tilings and Patterns* by Grünbaum/Shephard and *Quasicrystals and Geometry* by Marjorie Senechal with the exception of the first, which has been taken directly from Grünbaum/Shephard.

**2.3.1. Definition.** A **plane tiling** is a countable family of closed sets  $\mathcal{T} = \{T_1, T_2, \dots\}$  [...such that] the union of the sets  $T_1, T_2, \dots$  (which are known as the **tiles** of  $\mathcal{T}$ ) is to be the whole plane, and the interiors of the sets  $T_i$  are to be pairwise disjoint." (Grünbaum/Shephard, 16)

[One important part of this definition is that tilings are always infinite. The black and white square tiles in your bathroom cover the floor, but calling the pattern a tiling is technically incorrect, because tilings cover the entire plane.] With only the previous definitions, we still allow some unwanted configurations and tiles with bizarre shapes, such as the ones in figure 1.

To avoid this, we instate the following restriction.

**2.3.2. Restriction.** Let  $T_i, T_j$  be two tiles in  $\mathcal{T}$ . Then (a)  $T_i$  and  $T_j$  are each homeomorphic to a closed circular disk, and thus is a bounded, connected, and simply connected set, and (b)  $T_i \cap T_j = \{x\}$  is connected.

2.4. **Definition.** Let  $T_i \cap T_j = \{x\}$ . If  $x$  is a point in the plane, then  $x$  is called a **vertex**. If  $x$  is an arc, then  $x$  is called an **edge**. We will deal only with tiles that have a finite number of vertices and edges.

2.5. **Definition.** Let  $\mathcal{T}$  be partitioned into equivalence classes. Let  $\mathcal{P}$  be a set of representatives of these classes. We say that  $\mathcal{P}$  is a **protoset** for  $\mathcal{T}$ , and each representative is a **prototile**. We will only consider cases with finite protosets.

2.6. **Definition.** If a tiling,  $\mathcal{T}$  has protoset  $\mathcal{P}$ , then we say that  $\mathcal{P}$  **admits**  $\mathcal{T}$ .

2.7. **Definition.** A **patch** is a finite region of a tiling. More specifically, it is the union of a finite number of tiles such that the set is simply connected and will never become disconnected if a single point is deleted.

2.8. **Definition.** An arrangement of tiles is **locally legal** if the tiles are assembled in accordance with the relevant adjacency rules.

2.9. **Definition.** An arrangement of tiles is **globally legal** if it can be extended to an infinite tiling.

2.10. **Definition.** The **(first) corona** of a tile,  $T_i$  is the set  $\mathcal{C}(T_i) = \{T_j \in \mathcal{T} \mid T_i \cap T_j \neq \emptyset\}$ . We will use a slightly altered definition in the work that follows.  $\mathcal{C}(T_i) = \{T_j \in \mathcal{T} \mid T_i \cap T_j = \{x\} \text{ and } \exists y \subset \{x\} \mid y \text{ is an edge}\}$ . With this definition, tiles that share only a vertex with  $T_i$  are not included in its corona.

2.11. **Definition.** The **(first) corona atlas** is the set of all (first) coronas that occur in  $\mathcal{T}$ .

2.12. **Definition.** A **reduced (first) corona atlas** of  $\mathcal{T}$  is a subset of the corona atlas of  $\mathcal{T}$  that covers  $\mathcal{T}$ .

2.13. **Definition.** The **(first) vertex star** of a vertex  $v$  is the set  $\mathcal{S}(v) = \{T_j \in \mathcal{T} \mid T_j \cap v \neq \emptyset\}$ .

2.14. **Definition.** The **(first) vertex star atlas** is the set of all (first) vertex stars that occur in  $\mathcal{T}$ .

2.15. **Definition.** A tiling,  $\mathcal{T}$ , is **non-periodic** if it does not have translational symmetry in more than one direction.

2.16. **Definition.** A set of prototiles,  $\mathcal{P}$ , is **aperiodic** if all tilings it admits are non-periodic.

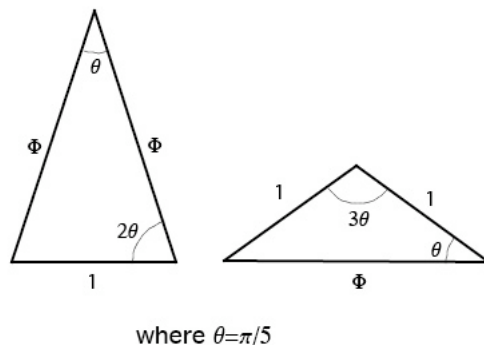


FIGURE 2. The two Penrose prototiles.

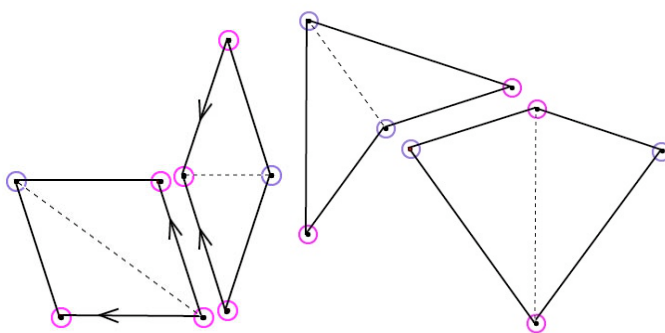


FIGURE 3. Left: adjacency rules for rhombs. Right: adjacency rules for kite and dart.

### 3. THE PENROSE APERIODIC TILES

Penrose Tilings are the most widely known tilings related to quasicrystals. These tilings cover the plane with just two distinct tiles. The first of these tiles is a triangle with angles  $\frac{1}{5}\pi$ ,  $\frac{1}{5}\pi$ , and  $\frac{3}{5}\pi$ , and the second is a triangle with angles  $\frac{2}{5}\pi$ ,  $\frac{2}{5}\pi$ , and  $\frac{1}{5}\pi$ . These isosceles triangles each have at least one side of length one and one side of length  $\Phi$ , where  $\Phi$  is the golden ratio:  $\Phi = \frac{1+\sqrt{5}}{2} = 1.618\dots$  [see Figure 3]

To form a Penrose tiling, the two types of isosceles triangles must be joined according to a set of adjacency rules.

**3.1. Adjacency Rules.** Two different sets of adjacency rules can be used to build a Penrose tiling with the aforementioned two triangles. The first is the kite and dart method, and the second is the rhombi method. Both of these are shown in figure 3. Remember that these adjacency rules ensure non-periodic tilings but do not determine the tiling; there are uncountably many distinct Penrose tilings.

3.1.1. *Rhombs.* Above, the adjacency rules for a tiling by rhombs are shown. Just as in the kite and dart tiling, the vertices of the individual tiles must be matched up according to color so that in the infinite tiling each vertex is a single color.

3.1.2. *Kite and Dart.* Below, the adjacency rules for a kite and dart tiling are shown. The vertices of the individual tiles must be matched up according to color (pink to pink and purple to purple) so that in the infinite tiling each vertex is a single color.

Note that there is a three dimensional analogue to the rhombs version of the Penrose tiling, but not of the other versions (Senechal, 170).

### 3.2. Two Properties of Penrose Tilings.

3.2.1. *Any finite pattern in a Penrose tiling is repeated infinitely many times in every infinite Penrose tiling.*

3.2.2. *There are uncountably many Penrose tilings.*

### 3.3. Determining the Index Sequence.

3.3.1. *Main Idea.* Here we state the general process of how to construct the index sequence, but a more detailed explanation is offered afterward. To form an index sequence of a Penrose Tiling,  $T$ , we will alter  $T$  by combining adjacent tiles to make larger tiles of the same shape. This is done by combining one acute triangle and one obtuse triangle to form a larger obtuse triangle, and combining two acute triangles and one obtuse triangle to form a larger acute triangle. The new triangles will be similar to the original ones, and the result will be another infinite Penrose Tiling with the tiles scaled by a factor of  $\Phi$ . [see Figure 4] As this process is iterated to infinity, the sequence,  $\{x_p\}$ , is determined at each step by the kind of triangle that contains  $P$ . A tiling can then be reconstructed from  $\{x_p\}$  that will be identical to the original tiling, except that it may be rotated based on the orientation of the starting triangle.

3.3.2. *Details.* (This is the method presented in Paterson, 165.) Consider a tiling that is made out of kites and darts. In this tiling, the long edges have length  $\Phi$ , and the short edges have length 1. Divide the two types of tiles down the middle, splitting each into two triangles. The dart will decompose into two obtuse triangles (with long edge of length  $\Phi$ , and short edges of length 1), and the kite will decompose into two acute triangles (with long edges of length  $\Phi$ , and short edge of length 1). Note that, as before,  $\Phi$  denotes the “golden number”:  $\Phi = (1 + \sqrt{5})/2 = 1.618\dots$

Let this tiling be  $T_n$ , let the smaller triangles (the obtuse ones, here) be  $S_n$ , and let the larger triangles (the acute ones) be  $L_n$ . Let  $P$  be a point in the plane tiled by  $T_n$ . If  $P$  is inside an element of  $L_n$ , the  $n^{\text{th}}$  number of the sequence is 0, and if it lies in an element of  $S_n$  the  $n^{\text{th}}$  number of the sequence is 1.

Next, we are going to form larger obtuse triangles by combining one obtuse triangle and one acute triangle using the following procedure. In each case where an acute triangle and an obtuse triangle share a short edge, delete that edge. This will give a new tiling,

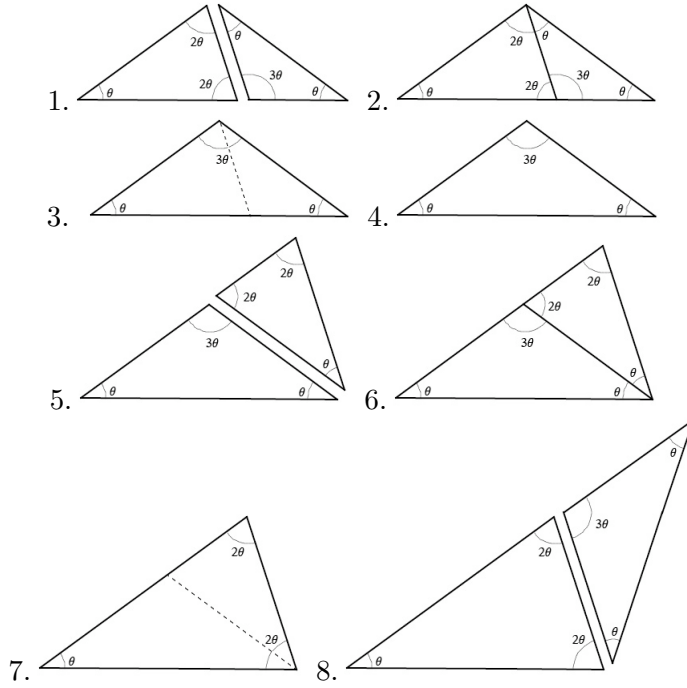


FIGURE 4. The amalgamating process for Penrose tiles.

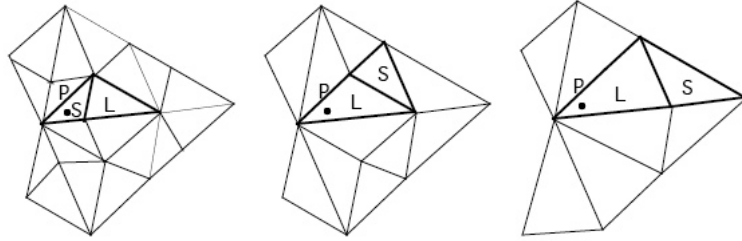
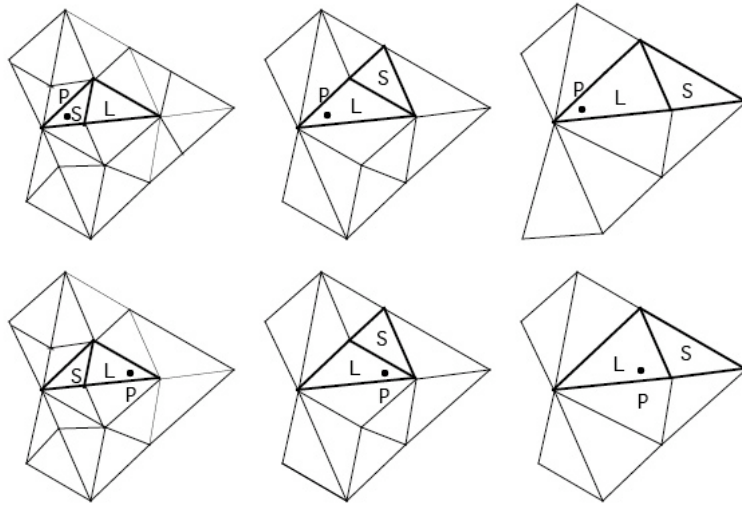
$T_{n+1}$  with a set  $S_{n+1}$  that consists of the remaining acute triangles of  $L_n$  and a set  $L_{n+1}$  consisting of the obtuse (newly constructed) triangles of  $T_{n+1}$ .

To find the next number in the index sequence for  $T$ , consider which type of triangle  $P$  is inside of in tiling  $T_{n+1}$ . If  $P$  is in an element of  $L_{n+1}$ , then the  $(n + 1)^{th}$  number in the sequence is 0, and if it lies in an element of  $S_{n+1}$  the  $(n + 1)^{th}$  number of the sequence is 1.

Now, we will do a similar process to form larger acute triangles. Whenever the short edge of an obtuse triangle (the larger kind in the previous tiling) corresponds to the long edge of an acute triangle (the smaller kind in the previous tiling), delete the edge. Now, we have a new tiling  $T_{n+2}$  with large (acute) triangles forming the set  $L_{n+2}$ , and small (obtuse) triangles forming the set  $S_{n+2}$ .  $T_{n+2}$  is a kite and dart tiling. In figure 3.3.2 we see this process carried out for a small patch of a Penrose tiling.

We generalize the iteration process as follows. We produce tiling  $T_{2n}$  from tiling  $T_{2n-1}$  by combining triangles of  $S_{2n-1}$  and triangles of  $L_{2n-1}$  whenever they share a short edge. Similarly, we produce tiling  $T_{2n+1}$  from tiling  $T_{2n}$  by combining a triangle of  $S_{2n}$  with a triangle of  $L_{2n}$  whenever they share an edge that is a long edge of the triangle in  $S_{2n}$  and the short edge of the triangle in  $L_{2n}$ . (Paterson, 165)

### 3.4. Forming a Groupoid.

FIGURE 5. A patch of a Penrose tiling with point  $P$  iterated twice.FIGURE 6. A patch of a Penrose tiling under two iterations shown with point  $P$  in two different locations.

3.4.1. *Defining the  $r$ -Discrete Equivalence Relation,  $R_p$ .* We define an equivalence relation,  $R_p$  on the set  $X_p$  of index sequences of Penrose tilings. (Note that  $X_p$  is the set of all sequences of zeros and ones, where a one is always followed by a zero. This must be the case, because in any tiling, the small triangles will be combined with large triangles to form the next tiling.) Let  $\{x_n\} \sim \{y_n\} \Leftrightarrow \exists m \mid x_n = y_n \forall n \geq m$ . More simply, two sequences are in the same equivalence class if they eventually coincide. This makes sense intuitively, because the choice of  $P$  is arbitrary, but as the sequence of tilings progresses, two different choices of  $P$  will eventually fall within the same triangle, and the sequences will be exactly the same from that point on [see Figure 3.4]. So, we have that the quotient space  $X_p/R_p$  is the set of all possible Penrose tilings, thereby making the choice of  $P$  insignificant.

Note that in the first three patches in figure 3.4, the point  $P$  begins in a small triangle, producing a sequence  $\{x\} = \{1, 0, 0, \dots\}$ . In the second series of three, the point  $P$  begins



in a large triangle, producing a sequence  $\{x\} = \{0, 0, 0 \dots\}$ . These two sequences coincide starting from the second term, which corresponds to the first iteration where the two points lie within the same triangle. (Paterson, 35, 165)

3.4.2. *Defining the Related  $r$ -Discrete Groupoid,  $G$ .* From the equivalence relation  $R_p$ , mentioned above, we use the standard method of defining a groupoid. Note, though, that not all groupoids are constructed from equivalence relations.

$$G = \{(x, y) \mid x \in X_p, y \in X_p, x \sim y\}$$

$$G^{(2)} = \{((x, y), (y, z)) \mid (x, y) \in G, (y, z) \in G\}.$$

\*Multiplication: For  $(x, y), (y, z) \in G$ , we define  $(x, y) \circ (y, z) = (x, z)$ .

$(x, y), (y, z) \in G \Rightarrow x \sim y$  and  $y \sim z$ . Since  $R_p$  is transitive,  $x \sim z$ , so  $(x, z) \in G$ .

\*Associativity:

$$((x, y) \circ (y, z)) \circ (z, w) = (x, z) \circ (z, w) = (x, w)$$

$$(x, y) \circ ((y, z) \circ (z, w)) = (x, y) \circ (y, w) = (x, w)$$

\*Identity Section:

$$\text{Let } r(x, y) = x, d(x, y) = y \forall (x, y) \in G.$$

$$\text{Define } \epsilon : X_p \rightarrow G \mid \epsilon(x) = (x, x).$$

We have that  $\epsilon(r(x, y)) \circ (x, y) = \epsilon(x) \circ (x, y) = (x, x) \circ (x, y) = (x, y)$ , and

$$(x, y) \circ \epsilon(d(x, y)) = (x, y) \circ \epsilon(y, y) = (x, y) \circ (y, y) = (x, y).$$

Therefore,  $\epsilon$  is the identity section of  $G$ .

\*Inversion:

$$\text{Let } (x, y)^{-1} = (y, x) \forall (x, y) \in G.$$

$$(x, y) \circ (x, y)^{-1} = (x, y) \circ (y, x) = (x, x) = \epsilon(r(x, y))$$

$$\text{and } (x, y)^{-1} \circ (x, y) = (y, x) \circ (x, y) = (y, y) = \epsilon(d(x, y))$$

#### 4. THE RELATED AMMANN TILING

Ammann Tilings cover the plane with three distinct tiles and can be derived from Penrose tilings. The work I have done with these tilings is original; only the description of their construction by Ammann (see: Grünbaum/Shephard, 548) was taken from the literature. My goal is to relate these tilings to quasicrystals by defining their related groupoid based on the method used in the Penrose case.

4.1. **Constructing the Tiling.** An Ammann tiling is constructed from a Penrose tiling by rhombs (we label these **type 1** and **type 2** for convenience; type 1 is shown above on the far left, and type 2 is to its right). Note that in the original Penrose tiling, the edges of the rhombs are all of equal length. The Penrose tiles must be assembled so that sides with matching markings (as shown in figure 4.1 are adjacent and properly oriented).

The construction of the Ammann tiling is determined entirely by the choice of point  $Q$ . The rest of the divisions of the rhombs are also shown in the diagram above such that lines that are the same length by construction are displayed in the same color. This construction is clearly unique once  $Q$  is chosen, because the triangle in the lower left of the type 1 rhomb above is congruent to the triangle on the lower left of the type 2 rhomb next to it. Similarly, the triangle on the upper right of the type 1 rhomb is congruent to

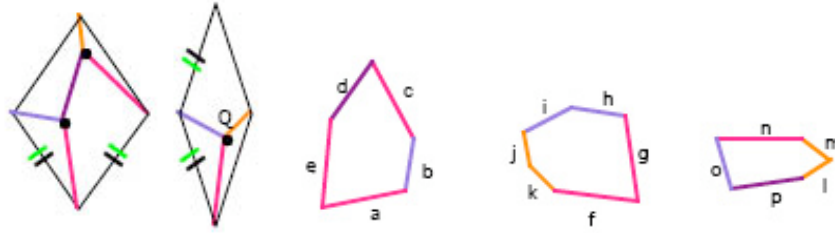


FIGURE 7. Left: the point  $Q$  and the resulting divisions of the two Penrose rhombs. Right: the resulting three Ammann tiles, A, B, and C.

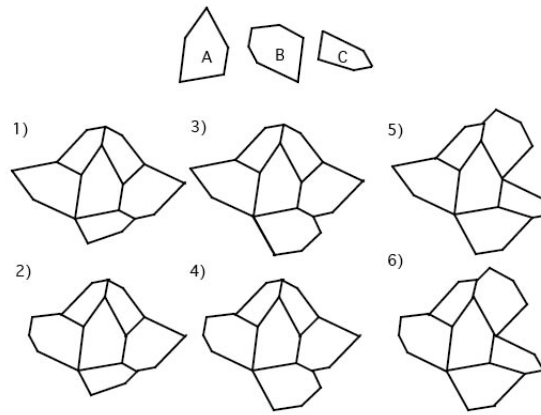


FIGURE 8. Above: the three Ammann prototiles. Below: the six coronas of  $A_n$

the triangle on the lower right of the type 2 rhomb. The dark purple line is constructed by joining the vertices of the two triangles that lie within the left rhomb.

In order to ensure a non-periodic tiling of the plane,  $Q$  must be chosen so that the distances from  $Q$  to the three vertices it is connected to and the distance between the two points in the interior of the type 1 rhomb are all different (Grünbaum/Shephard, 548). More simply, the segments shown above in pink, orange, light purple, and dark purple are all of different lengths. As the color-coding in figure 4.1 suggests, the construction of the

$$\text{Ammann tiles necessarily causes } \begin{cases} a = c = e = f = g = n \\ b = h = i = o \\ j = k = l = m \\ d = p \end{cases} .$$

**4.2. Iterating Tilings.** Just as with a Penrose tiling, it is possible to create an index sequence for an Ammann tiling. In order to clarify the process of going from  $T_n$  to  $T_{n+1}$ ,

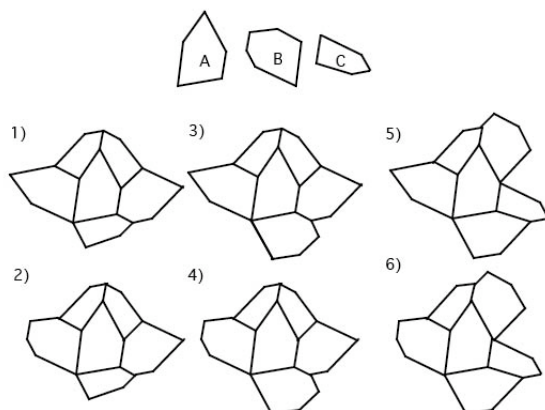


FIGURE 9. Above: the three Ammann prototiles. Below: the six coronas of  $A_n$

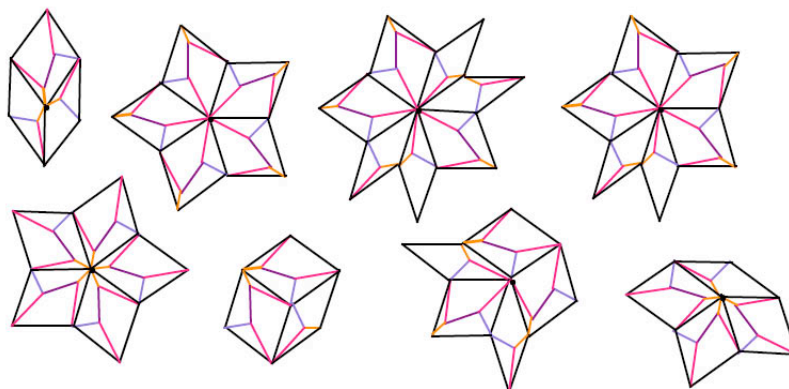


FIGURE 10. The eight vertex stars of the Penrose vertex star atlas (Senechal, 177)

we label the pentagon in  $T_n$  with three sides of equal length type  $A(n)$ , the hexagon type  $B(n)$ , and the other pentagon type  $C(n)$ .

4.3. **Theorem 1.** Given an Ammann tiling,  $T_n$ , the six coronas illustrated in figure 4.2 are the only possible coronas of an  $A(n)$  tile (the only possible arrangements of tiles of  $T_n$  around  $A(n)$ ) for any  $n \in \mathbb{N}$ .

4.4. **Proof.** Let  $T_n$  be an Ammann Tiling. There is necessarily a Penrose tiling by rhombs that corresponds to  $T_n$ .

As can be seen by inspection of figure 10, a type 1 rhomb of the Penrose tiling is needed to form a type  $A$  tile in the corresponding Ammann tiling. So, to look at all possible

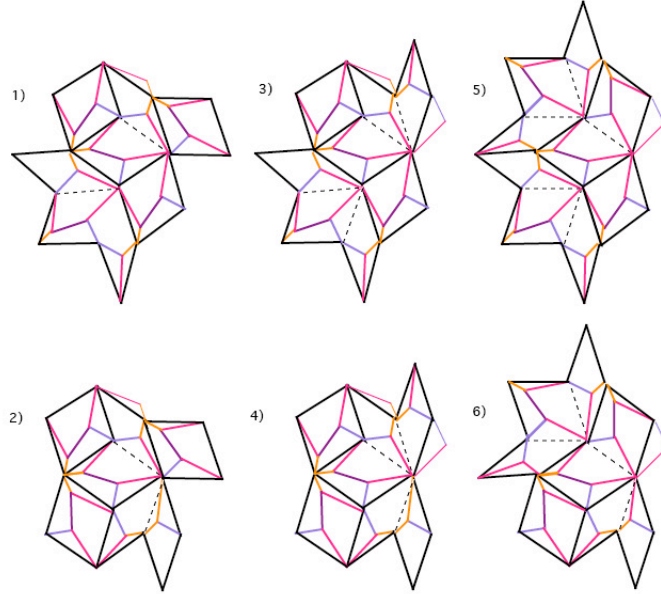


FIGURE 11. The six Penrose coronas of a type 1 rhomb with colored Ammann divisions.

Ammann coronas of  $A$ , we must look at all possible Penrose coronas of a type 1 rhomb [see Figure 11].

The same images again in figure 12, with only the relevant lines colored.

As you can see, the six possible coronas of a type 1 rhomb yield exactly six possible coronas of the corresponding type  $A$  tile (the ones we wanted). Therefore, these six coronas are the only possible coronas of  $A$ .

4.5. **Theorem 2.** The set of Ammann coronas of  $A$  is a reduced corona atlas.

4.6. **Proof.** We will use proof by contradiction. Assume that the set of coronas of  $A$  does not cover the tiling. Then, there is at least one corona of a  $B$  or  $C$  tile that does not contain any  $A$  tiles. Consider the corresponding Penrose tiling. As stated above, a type 1 rhomb necessarily results in a type  $A$  tile. So, the corresponding Penrose patch does not have any type 1 rhombs. Note that for an Ammann patch of  $n$  tiles, the corresponding Penrose patch contains at least  $n$  tiles. This means that there exists a patch in the Ammann tiling of at least six tiles, none of which is type  $A$ . Furthermore, the corresponding Penrose patch contains at least six type 2 (skinny) rhombs and no type 1 rhombs. But consider the Penrose vertex star atlas (Figure 10).

The Penrose vertex star atlas determines every Penrose tiling (Senechal, 177). Note that in each vertex star there is at least one type 1 rhomb. So, we have reached a contradiction. Therefore, this set of four coronas of type  $A$  tiles covers the tiling, and is thus a reduced corona atlas.

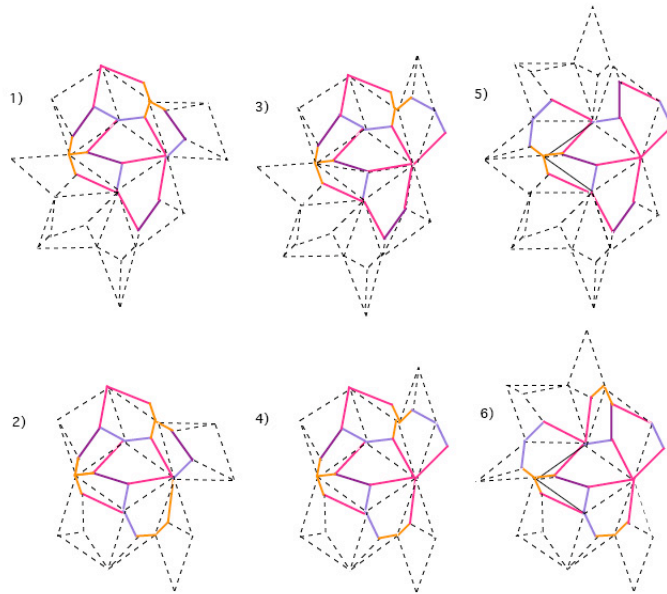


FIGURE 12. The six Penrose coronas of a type 1 rhomb with only the Ammann coronas of the central  $A$  tile colored.

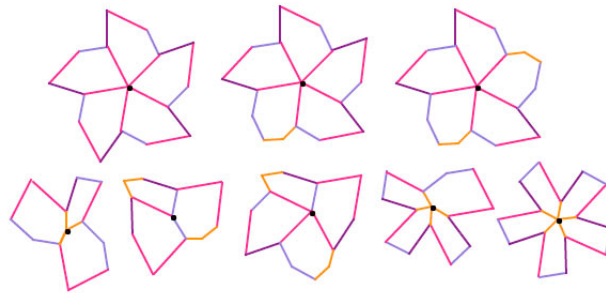


FIGURE 13

4.7. **Theorem 3.**  $A$ ,  $B$ , and  $C$  are an aperiodic protoset.

4.8. **Proof.** From the Penrose vertex atlas, we get the eight Ammann vertex stars shown in figure 13.

Using the angle numbering from figure 4.8, we find from the first eight vertex stars:

$$\begin{cases} 5 = 6 = 12 = 2\theta \\ 8 = 10 = 4\theta \\ 2 + 14 = 6\theta \end{cases}$$

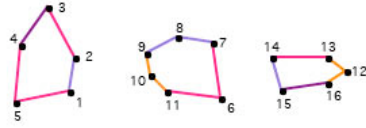


FIGURE 14

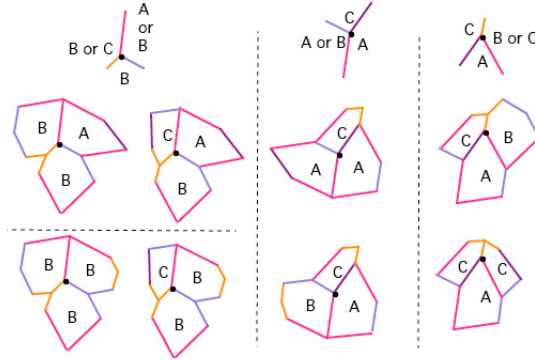


FIGURE 15

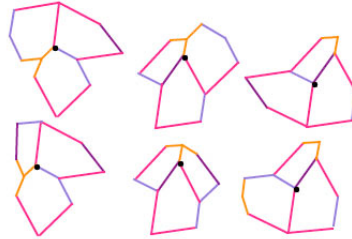


FIGURE 16. The additional six globally legal Ammann vertex stars.

But since the construction of the Ammann tiles added three vertices, we need to consider the vertex stars of these. The neighborhoods of  $A$  determined in Theorem 1 yield the ten locally legal vertex stars shown in figure 18. Of these,  $(B,B,B)$  and  $(C,B,B)$  are not globally legal because there is no vertex with angle  $2\theta$  that is connected to two purple edges. Note that vertex star  $(B,B,B)$  corresponds to incident vertices  $(7,11,9)$  and  $(C,B,B)$  corresponds to  $(7,13,9)$ . The other six can be seen in the marked Penrose coronas of type 1 tiles seen earlier. So, we have six more globally legal Ammann vertex stars (Figure 16).

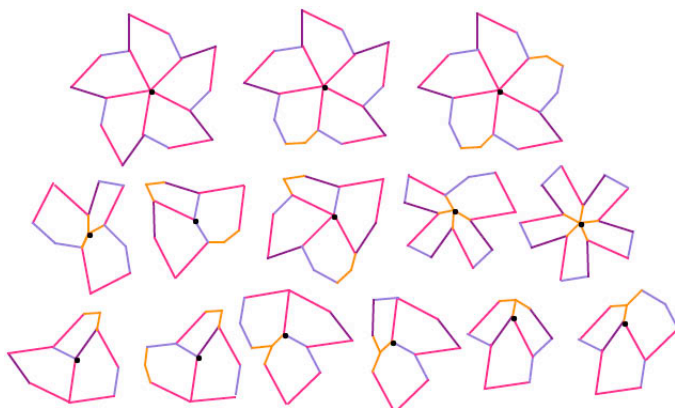


FIGURE 17

From these six, we get the following angle relations. 
$$\left\{ \begin{array}{l} 1 = 7 \\ 11 = 13 \\ 3 + 13 + 16 = 10\theta \\ 4 + 15 + 7 = 10\theta \\ 1 + 9 + 11 = 10\theta \end{array} \right.$$

Combining these sets, we have fourteen vertex stars that appear in an Ammann tiling that has been derived from a Penrose tiling by rhombs. These thirteen necessarily appear in the Ammann vertex star atlas.

So, the angle relations that result from construction are: 
$$\left\{ \begin{array}{l} 5 = 6 = 12 = 2\theta \\ 8 = 10 = 4\theta \\ 2 + 14 = 6\theta \\ 3 + 13 + 16 = 10\theta \\ 4 + 15 + 7 = 10\theta \\ 1 + 9 + 11 = 10\theta \\ 1 = 7 \\ 11 = 13 \end{array} \right.$$

With these angle relations and the known edge congruences, there are ten more possible vertex stars, which are shown below. (We leave as an exercise the proof that there are no other locally legal Ammann vertex stars.) The central vertex of each vertex star is labeled with the numbers of the vertices that meet there.

We prove that none of these ten vertex stars can be extended to an infinite tiling:

We have already shown that (7,13,9) and (7,11,9) are not globally legal. If two instances of vertex 6 meet, then vertices 7 and 11 meet. But if vertices 7 and 11 meet, then vertex 9 meets there as well, because  $7 + 11 = 10\theta - 9$ . However, as stated above, (7,11,9) is not globally legal, so a vertex star where two instances of vertex 6 meet is not globally legal.

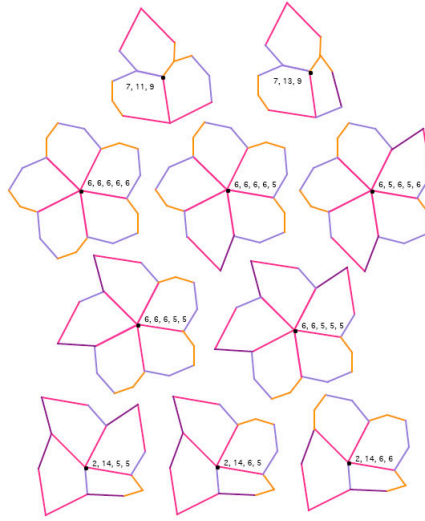


FIGURE 18

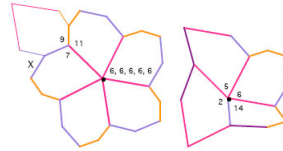


FIGURE 19

Therefore,  $(6,6,6,6,6)$ ,  $(6,6,6,6,5)$ ,  $(6,6,6,5,5)$ ,  $(6,6,5,5,5)$ ,  $(6,5,6,5,6)$ , and  $(2,14,6,6)$  are not globally legal.

Now, we focus our attention to vertex  $(2,14,6,5)$ . We have already shown that there are only six possible coronas of an A tile. But the configuration of the vertex star of  $(2,14,6,5)$  does not fit with any of these. Specifically, two A tiles may not be placed so that vertices 5 and 2 are incident.

So,  $(2,14,6,5)$  and  $(2,14,5,5)$  are not globally legal. Therefore, none of these ten vertex stars is globally legal, and Ammann vertex star atlas contains only the aforementioned fourteen vertex stars.

The Penrose vertex star atlas of eight vertex stars completely determines all Penrose tilings (Senechal, 177). So, the set of fourteen Ammann vertex stars that are derived from a Penrose tiling completely determines all Ammann tilings that can be derived from Penrose tilings. But the set of vertex stars of an Ammann tiling that has been derived from a Penrose tiling is identical to the vertex star atlas of an arbitrary Ammann tiling. Therefore, an arbitrary Ammann tiling can be derived from a corresponding Penrose tiling.



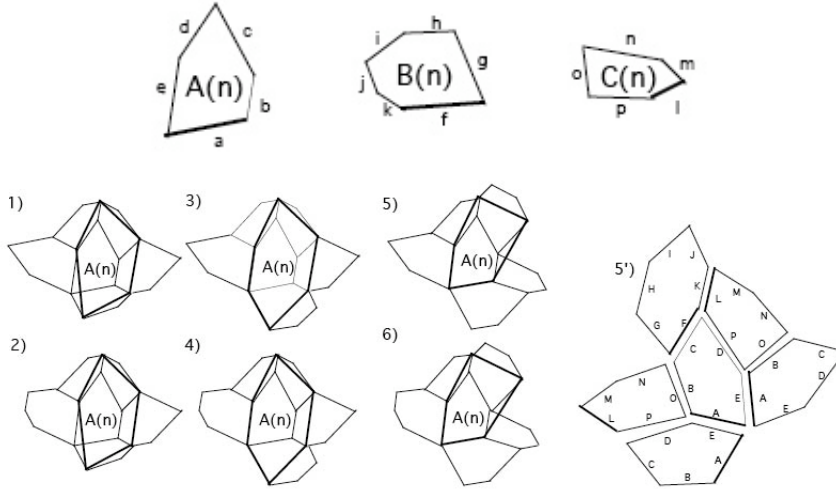


FIGURE 20. Top: the prototiles of  $T_n$  with main edges shown in bold. Bottom left: the six coronas of  $A_n$  tiles with constructed edges shown bold. Bottom right: the tiles of  $T_{n+1}$  arranged around an  $A_{n+1}$  tile in configuration 5) with main edges bold.

Since Penrose tilings are non-periodic, so too are Ammann tilings. Therefore, A, B, and C form an aperiodic protoset.

**4.9. Construction Algorithm.** By connecting vertices within the six coronas of  $A_n$  as shown in figure 20, we create a new set of three tiles. We label the new tiling  $T_{n+1}$  and label the new tiles  $A_{n+1}$ ,  $B_{n+1}$ , and  $C_{n+1}$ . (Eventually, we will show that tiling  $T_{n+1}$  is an Ammann tiling with protoset  $\{A_{n+1}, B_{n+1}, C_{n+1}\}$ .)

To clarify the labeling of the diagram: the edges of type A tiles are labeled with letters  $a$  through  $e$ , type B tiles are labeled with letters  $f$  through  $k$ , and type C tiles are labeled with letters  $l$  through  $p$ . The *main edge* is shown below in bold in each case where the tiles are shown separately and always carries the label of the earliest alphabetical letter. More explicitly, type A tiles have main edge labeled  $a$ , type B tiles have main edge labeled  $f$ , and type C tiles have main edge labeled  $l$ . In the new tiling, the labeling proceeds alphabetically in the opposite direction.

Figure 20 shows the construction used to proceed from  $T_n$  to  $T_{n+1}$ .

In figure 20 both (1) and (2) form tiles of type  $A_{n+1}$ , (3) and (4) form tiles of type  $B_{n+1}$ , and (5) and (6) form tiles of type  $C_{n+1}$ .

A proof will be given shortly that the corona atlas of  $T_{n+1}$  is the same form as the corona atlas of  $T_n$ , but for now, you can see that this is a plausibly claim by looking at corona (5') in figure 20, which shows the tiles of  $T_{n+1}$  assembled as a corona of an  $A_{n+1}$  tile.

**4.10. Theorem 4.** Let  $T_n$  be an Ammann tiling. Then, under the algorithm mentioned above,  $T_{n+1}$  is also an Ammann tiling. We will do this by proving the following:

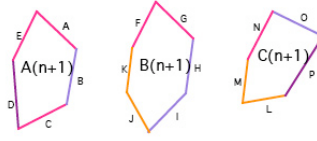
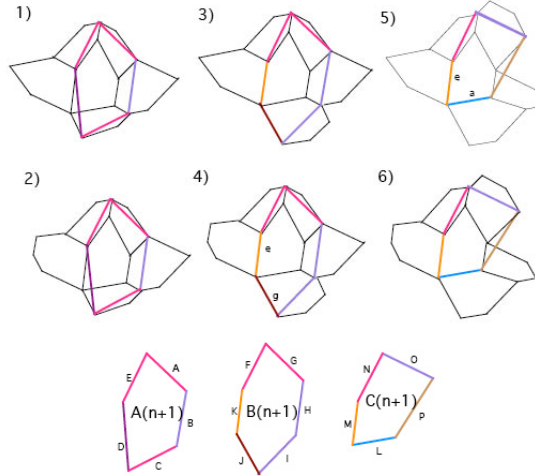


FIGURE 21

- (a) Edge congruences are conserved from  $T_n$  to  $T_{n+1}$ .
- (b)  $T_{n+1}$  has the same corona atlas (its tiles fit together in the same way) as  $T_n$ .
- (c) We can construct a tiling of 2 rhombs from the vertices of  $T_{n+1}$ .
- (d) This tiling is a Penrose tiling.

4.11. **Proof of (a).** Since  $T_n$  is an Ammann tiling,  $a = c = e = f = g = n$ ,  $b = h = i = o$ ,  $j = k = l = m$ , and  $d = p$ . By construction, as shown in the picture below,  $A = C = E = F = G = N$ ,  $B = H = I = O$ ,  $K = M$  in tiling  $T_{n+1}$ .



Since in  $T_n$ ,  $a = e = g$ , we have  $J = K = M = L$ . Also, it can be easily shown that only an  $A$  tile would fit between the  $C$  and  $B$  tiles on the right in figures (1) and (2), so  $D = P$ .

Therefore, (keeping in mind that the edges of the new tiling are labeled in the opposite direction) we get the edge congruences shown below:  $A = C = E = F = G = N$ ,  $B = H = I = O$ ,  $J = K = M = L$ ,  $D = P$ .

So, the algorithm preserves congruence of edges between  $T_n$  and  $T_{n+1}$ .

4.12. **Proof of (b).** Clearly, the angles of  $T_n$  are not congruent to the angles of  $T_{n+1}$ . We want to show that the restrictions imposed by our algorithm for constructing  $T_{n+1}$  are the same as the restrictions present in  $T_n$ .

In proving Theorem 2, we came up with the Ammann vertex atlas shown in figure 22.

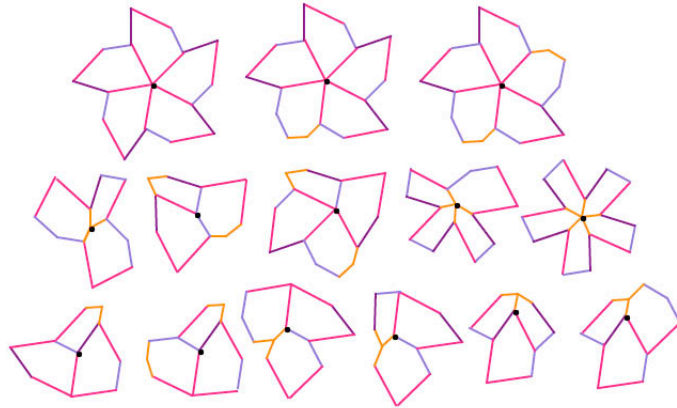


FIGURE 22

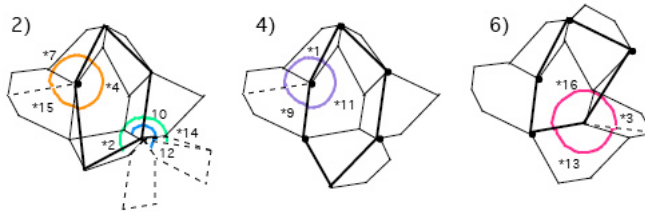


FIGURE 23

And we arrived at the following angle relations for  $T_n$ :

$$\left\{ \begin{array}{l} 5 = 6 = 12 = 2\theta \\ 8 = 10 = 4\theta \\ 2 + 14 = 6\theta \\ 3 + 13 + 16 = 10\theta \\ 4 + 15 + 7 = 10\theta \\ 1 + 9 + 11 = 10\theta \\ 1 = 7 \\ 11 = 13 \end{array} \right.$$

Now, we show that the construction algorithm gives us exactly the same restrictions on  $T_{n+1}$ .

In the picture below, we label the interior angles by the corresponding vertex labels.

From this picture, we get immediately:  $*12 = 5 = 2\theta$ ,

$*5 = *6 = 12 = 2\theta$ ,

$*8 = 10 = 4\theta$ ,

$*10 = 5 + 6 = 4\theta$ ,

$*11 = *13$ , and

$$*1 = *7$$

Look at the vertex circled in orange to see:  $*4 + *7 + *15 = 10\theta$ .

Look at the vertex circled in pink to see:  $*3 + *13 + *16 = 10\theta$ .

Look at the vertex circled in purple to see:  $*1 + *9 + *11 = 10\theta$ .

Now, look at vertex  $*2$ . The green arc marks angle  $*2$  and the blue arc marks angle  $*14$ . Also, the purple arc marks angle  $10 = 4\theta$ , and the brown arc marks angle  $12 = 2\theta$ .

So,  $*2 + *14 = 10 + 12 = 6\theta$ .

$$\text{The angle restrictions are: } \begin{cases} 5 = *6 = *12 = 2\theta \\ *8 = *10 = 4\theta \\ *2 + *14 = 6\theta \\ *3 + *13 + *16 = 10\theta \\ *4 + *15 + *7 = 10\theta \\ *1 + *9 + *11 = 10\theta \\ *1 = *7 \\ *11 = *13 \end{cases}$$

These are exactly the same angle relations present in  $T_n$ . Since angle relations are conserved from  $T_n$  to  $T_{n+1}$  and length congruences are conserved as well (by (b)),  $T_{n+1}$  has the same corona atlas (and reduced corona atlases) as  $T_n$ .

**4.13. Proof of (c).** Since  $T_n$  is an Ammann tiling, it has a unique corresponding Penrose tiling. Figure 24 shows the coronas of  $A_n$  with the corresponding Penrose tiles drawn in, and directly below are the tiles of  $T_n$  with numbered vertices and black lines drawn where they are cut by possible corresponding Penrose tiles. The multiple labels at a vertex indicate the two or three vertices that coincide there.

Now, in order to make a tiling by rhombs that corresponds to  $T_{n+1}$ , we note the label numbers of the vertices that are connected in  $T_n$  and connect the corresponding vertices in  $T_{n+1}$ . In figure 26 the three tiles of  $T_{n+1}$  are drawn with these cuts and are superimposed upon the four Amman coronas.

From figure 25, we see that the segments  $\overline{6,10}$  and  $\overline{12,14}$  (shown in light blue) are of equal length by construction. Similarly,  $\overline{2,5}$  and  $\overline{6,8}$  (shown in green) are the same length.

Figure 25 shows corona (4) redrawn with the blue line, the green line, and some length labels. Note that both rhombs have all sides of length  $\Phi$ .

The green line is clearly of length  $\Phi + 1$ . We determine the length of the blue line by using the law of cosines ( $c^2 = a^2 + b^2 - 2ab \cos C$ ):

$$X = \sqrt{\Phi^2 + \Phi^2 - 2\Phi^2 \cos \frac{3}{5}\pi}$$

$$X = \sqrt{2\Phi^2 - 2\Phi^2 \cos \frac{3}{5}\pi}$$

$$X = \Phi \sqrt{2 - 2 \cos \frac{3}{5}\pi}$$

$$X = \Phi(\Phi)$$

$$X = \Phi^2 = \Phi + 1$$

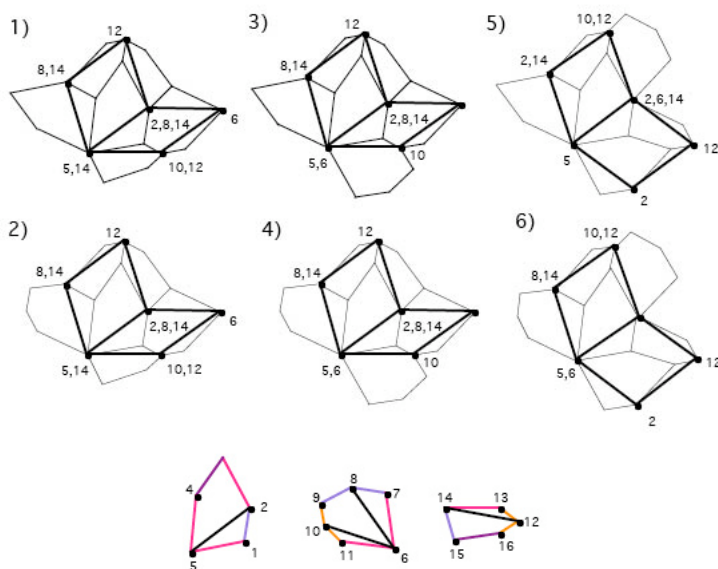


FIGURE 24

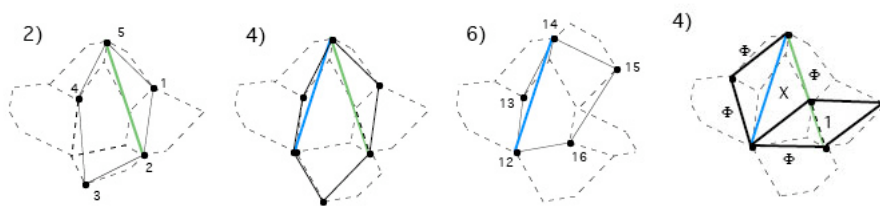


FIGURE 25

So, the blue and green lines are the same length, giving us:  $\overline{6,10} = \overline{12,14} = \overline{2,5} = \overline{6,8}$ . Since we have already shown that the  $T_{n+1}$  tiles assemble themselves in exactly the same patterns as the  $T_n$  tiles, we cut the new tiling along these lines and have produced a tiling by rhombi.

**4.14. Proof of (d).** Note that rhombs have opposite angles equal. Let the small angle of a 1rhomb (the rhomb corresponding the the Penrose “fat rhomb”) be  $x$ , and let the large angle be  $y$ . Let the small angle of a 2rhomb be  $z$ , and let the large angle be  $w$ .

Since we know that the  $T_{n+1}$  tiles fit together in the same patterns as the  $T_n$  tiles, we extend corona (5) of  $T_{n+1}$  as shown in figure 27. Since five identical 1rhombs are need to complete the cycle of  $2\pi$  with angle  $x$  in the center,  $x = \frac{2}{5}\pi$ . So,  $y = \frac{3}{5}\pi$ . Therefore, 1rhombs are Penrose type 1 rhombs.

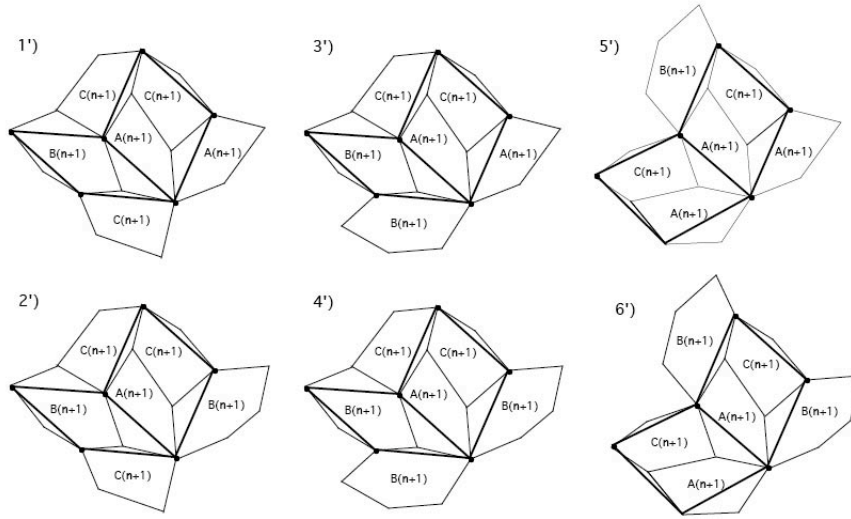


FIGURE 26

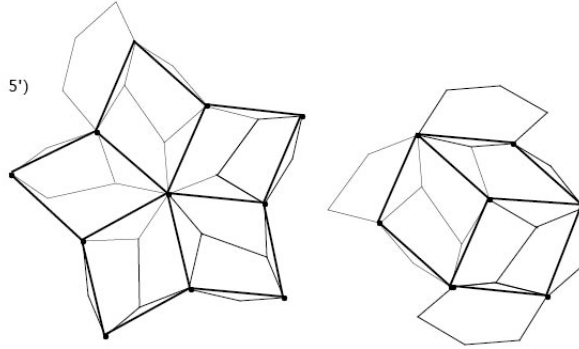


FIGURE 27

Since,  $T_{n+1}$  and  $T_n$  have the same corona atlas, the configuration shown in figure 27 is valid. Here, the large angle of the 2rhomb supplements the sum of two large angles of 1rhombs.  $2y + w = 2\pi \Rightarrow w = 2\pi - (2)\frac{3}{5}\pi = \frac{4}{5}\pi$ , and the last vertex is:  $z = \pi - \frac{4}{5}\pi = \frac{\pi}{5}$ . Therefore, 2rhombs are Penrose type 2 rhombs.

Since 1rhombs are Penrose type 1 rhombs, and 2rhombs are Penrose type 2 rhombs, the tiling from part (c) is a Penrose tiling. Therefore,  $T_{n+1}$  is an Ammann Tiling.

## 5. FORMING AN INDEX SEQUENCE

**5.1. Why don't we model the index sequence on the Penrose case?** We still have not determined a method for encoding the information in an Ammann tiling into a

sequence. In the process of iterating a Penrose tiling (by triangles) edges are deleted, but never added, which is essential to the iteration process. This ensures that two points in the same triangle will be in the same triangle in every subsequent iteration of the tiling. Unfortunately, the process described above for iterating an Ammann tiling, each iteration adds and deletes edges. Identical Penrose index sequences are constructed whenever two points  $P_1$  and  $P_2$  lie within the same tile of the original tiling. In the Ammann case, something very different happens: when the tiling is iterated, a new edge may divide a tile, so although  $P_1$  and  $P_2$  start out in the same tile of  $T_1$ , they may not lie in the same tile of  $T_2$ . Whenever this is the case, the index sequences of  $T_1$  corresponding to  $P_1$  and  $P_2$  are not identical (they differ in at least one digit), and it is extremely difficult to determine whether  $\exists m \in \mathbb{N} \mid x_n = y_n \forall n > m$ , where  $x_n$  is the index sequence corresponding to  $P_1$  and  $y_n$  is the index sequence corresponding to  $P_2$ . But since the index sequences track the same tiling, we need them to agree eventually.

**5.2. Forming the Groupoid.** Our goal is to construct a groupoid just as we did in the Penrose case and define an equivalence relation,  $R_m$  on this set:  $\{x_n\} \sim \{y_n\} \Leftrightarrow \exists m \mid x_n = y_n \forall n > m$ . Once we have the process for determining the index sequence  $\{x\}$  of a tiling, this is a very natural procedure.

From this equivalence relation, we construct a groupoid just as we did for Penrose Tilings.

## 6. DIFFERENCES BETWEEN PENROSE AND AMMANN TILINGS

\*The process for iterating an Ammann tiling creates new edges, while the process for iterating a Penrose tiling does not. (Neither process creates new vertices.)

\*Ammann tiles have no adjacency rules for assembly (though they will only fit together in certain configurations). Penrose tiles have marked vertices and edges to indicate proper assembly.

\*No matter what the size of the tiling, Penrose tiles are always similar to the original two tiles (though they may each have a different scaling factor). Ammann tiles preserve all of the edge congruences, but only some of the angle congruences as the tiling is iterated. It is not yet determined whether some of the iterations involve similar tiles. It is clear, though, that the differences in tile shape between iterations are not correlated to the differences between the kite and dart method vs. the rhombs method for Penrose tilings, because an Ammann tiling can only be constructed from a tiling by rhombs, so each iteration of the Ammann tiling corresponds to two iterations of the original Penrose tiling.)

\*It is not known whether the Ammann tiling is useful in studying quasicrystals.

## 7. WHAT ELSE IS LEFT TO DO?

\*What is the relationship between the tiles in  $T_n$  and  $T_{n+1}$ ?

\*Are  $T_n$  tiles similar to  $T_{n+2}$  tiles?

\*Is there a bijection between  $X_p$ , the set of all sequences that represent Penrose tilings, and  $X_m$ , the set of sequences that represent Ammann tilings?

## 8. WORKS CITED

*Tilings and Patterns* by Grünbaum/Shephard.

*Quasicrystals and Geometry* by Marjorie Senechal.

*Groupoids, Inverse Semigroups, and Their Operator Algebras* by Alan L.T. Paterson